

Covalent Triazine Framework as Catalytic Support for Liquid Phase Reaction

Carine E. Chan-Thaw,[†] Alberto Villa,[‡] Phisan Katekomol,[†] Dangsheng Su,[§] Arne Thomas,^{*,†} and Laura Prati[‡]

[†]Technische Universität Berlin, Englische Strasse 20, 10587 Berlin, Germany, [‡]Dipartimento di Chimica Inorganica Metallorganica e Analitica, Università degli Studi di Milano, via Venezian 21, 20133 Milano, Italy, and [§]Inorganic Chemistry department, Fritz Haber Institute der Max Planck Gesellschaft, Faradayweg 4-6, 14195 Berlin, Germany

ABSTRACT An important goal in the preparation of highly active supported metal particles is the enhancement of the metal support interaction, providing a more stable catalyst, especially for liquid phase reactions as the leaching and reconstruction of the active phase causes deactivation. In this work, a covalent triazine framework (CTF) as support for Pd nanoparticles is compared to activated carbon (AC), the typical support used in liquid phase reactions. The results indicate that the presence of the N-heterocyclic moieties on the surface of the frameworks is beneficial for improving the stability of Pd nanoparticles during the liquid phase glycerol oxidation. Pd/CTF showed better activity and in particular better stability when compared to Pd supported on activated carbon (AC).

KEYWORDS Porous polymer framework, palladium, liquid phase oxidation, glycerol

The development of new supports for the immobilization of metal nanoparticles as catalyst for liquid phase reactions has been recently the subject of growing interest.¹ A solution for enhancing the catalytic performance and the stability of these systems is the introduction of functional, for example nitrogen groups, on the surface of the support. Jiang et al. observed that the introduction of nitrogen functionalities on the surface of carbon nanotubes^{2,3} (CNTs) increases the dispersion and the stability of gold nanoparticles. The homogeneous distribution of gold nanoparticles was enabled by the strong interaction with the nitrogen-doped carbon nanotubes. Nitrogen-doped CNTs supported metal nanoparticles show better activity than pristine CNTs when used as catalyst for the Heck reaction of iodobenzene and styrene⁴ and the cinnamaldehyde hydrogenation.⁵ The cinnamaldehyde hydrogenation into hydrocinnamaldehyde was successful also on nitrogen-doped CNTs using palladium as the active phase.⁶ More recently, mesoporous nitrogen containing carbon nanoparticles were reported highly active in the base-catalyzed transesterification of β -keto esters of aryl, aliphatic, and cyclic primary alcohols.⁷

Another class of materials, which have been recently investigated as support, are metal organic frameworks (MOFs) exhibiting high surface area and tunable pore size.⁸ The versatile coordination chemistry and polytopic linkers allow for the design of unlimited structures of MOFs. When functionalized with amino groups, MOFs are active in the Knoevenagel condensation of benzaldehyde with ethyl cy-

anoacetate and ethyl acetoacetate,⁹ Aza-Michael condensation and ethyldecanoate transesterification.¹⁰ Some groups investigated metal incorporation into MOF. Hermes et al.¹¹ successfully loaded metals into MOFs by chemical vapor deposition. Hwang et al.¹² proposed the incorporation of palladium by ionic exchange after amine grafting onto coordinatively unsaturated metal sites of MOF. The generation of silver and gold nanoparticles in situ was tried by Moon et al.¹³ within a flexible nickel-containing MOF. Metal-containing MOFs have also been extensively considered as support for catalysis in liquid phase reactions.^{14–17} Palladium particles supported on MOF-5 catalyzed the hydrogenation of ethyl cinnamate without any observation of palladium leaching, as well as the hydrogenation of styrene, 1-octene and *cis*-cyclooctene.¹⁸ We recently developed a new class of covalent organic frameworks that are formed by the trimerization of aromatic nitriles in molten ZnCl₂.^{19–22} CTFs exhibit very high surface areas and high amounts of nitrogen functionalities in the networks. Because of the fully covalent structure, they possess an increased thermal and chemical stability, making them interesting candidates as new catalyst supports in liquid phase reactions.

Indeed, CTFs have recently shown to be highly stable even at harsh conditions. Palkovits et al.²³ applied a CTF loaded with a platinum salt as catalyst for methane oxidation in concentrated sulfuric acid at 215 °C. The catalyst and the CTF support showed no detectable degradation even after several reaction cycles. We report herein, the application of CTFs as support for Pd nanoparticles for the liquid phase oxidation of glycerol. This reaction is typically carried out in the presence of dioxygen as the oxidant and different authors report the use of Au, Pd, and bimetallic systems on activated carbon (AC) as the catalytic system.^{24–27} Under such conditions, Pd supported on AC suffers from severe

* To whom correspondence should be addressed. E-mail: arne.thomas@tu-berlin.de.

Received for review: 10/9/2009

Published on Web: 01/19/2010



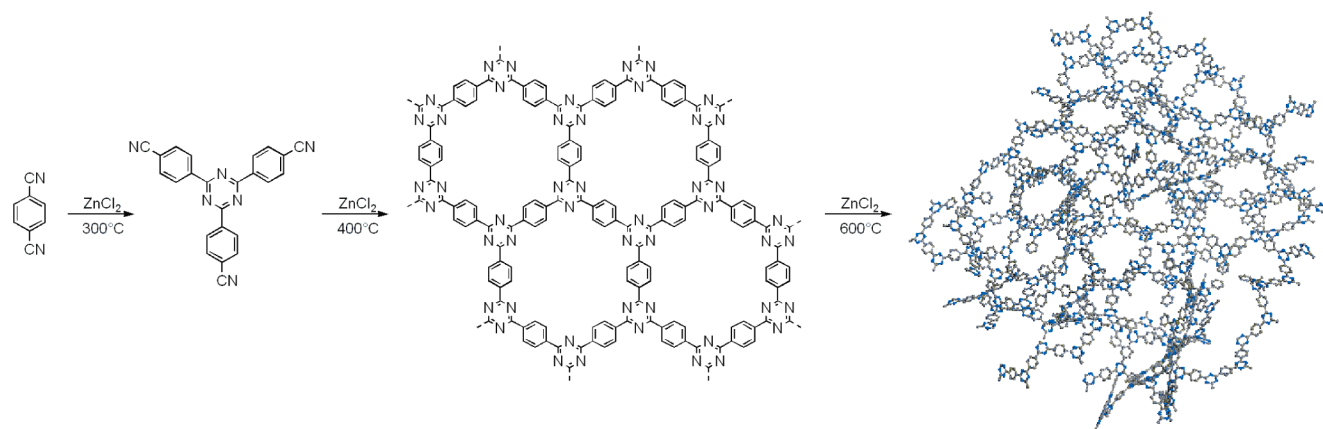


FIGURE 1. Reaction scheme of the dynamic trimerization of terephthalonitrile leading to the formation of a 2D framework. At 400 °C, an organized triazine network is formed whereas at 600 °C an amorphous network is obtained.

deactivation, which is ascribed to the following factors: metal sintering and/or segregation, leaching, irreversible adsorption, and overoxidation.²⁵

The use of CTFs as support for Pd-NPs, could represent an advantage in terms of metal–support interactions that in turn could modify and possibly improve the resistance of the catalyst.

The CTF support was synthesized using 1,4-dicyanobenzene and ZnCl_2 in a molar ratio of 1:5. This mixture is transferred to a sealed quartz ampule and heated to 400 and 600 °C. During the first temperature step (400 °C) an organized triazine network is formed, which is reorganized at the second higher temperature step (600 °C), involving CN eliminations and irreversible condensation reactions into an amorphous network (Figure 1). Indeed, at 600 °C opening triazine cross-links is leading to local expansions of the network.^{20–22} This reorganization yields on the one hand a decrease of the overall nitrogen content, from 20 wt % for the ideal CTF structure to 10 wt % for the CTF heated to 600 °C. On the other, a hierarchical pore structure is formed exhibiting mesopores beside micropores and surface area and pore volume increase to a large extent in these amorphous networks.

After the reaction, the ZnCl_2 is removed by extensive washing with water (0.3 wt % Zn remains checked by inductive coupled plasma, ICP). The CTF was dried and carefully grinded before the application of the metal nanoparticles.

Pd/AC (1 wt %) and 1 wt % Pd/CTF were synthesized via the sol immobilization technique (NaBH_4/PVA).²⁸ The palladium metal sol was generated by NaBH_4 reduction of Na_2PdCl_4 salt in the presence of a protective agent (polyvinyl alcohol, PVA) which provides electrostatic as well as sterical stabilization of the nanoparticles. In principle, the immobilization of preformed Pd nanoparticles assured a similar particle size distribution on different support. To study a possible contribution of Zn as catalytic metal in the liquid phase oxidation, additional Zn was added to the support (1.3 wt % determined by ICP) and on the modified CTF, Pd NPs were immobilized.

TABLE 1. Characterization of the Samples (Activated Carbon X40S, CTF, and Pd/CTF) by Nitrogen Sorption Measurements and Combustion Elemental Analysis

	surface area ($\text{m}^2 \text{g}^{-1}$)	pore volume ($\text{cm}^3 \text{g}^{-1}$)	elemental analysis (wt %)		
			C	N	H
CTF	2814	1.79	71	9.0	0.9
X40S	1100	1.50	80	0.3	0.3
1 wt % Pd/CTF	2490	1.56	67	9.0	0.9

CTF and Pd/CTF were characterized by X-ray diffraction (XRD), nitrogen sorption measurements, and combustion elemental analysis. As expected, the CTF and Pd/CTF are fully amorphous. The diffractograms of the Pd/CTF before and after the catalytic reaction show a broad peak at $2\theta = 26^\circ$ corresponding to an average distance of 3.4 Å showing a partial stacking of aromatic units and a peak at $2\theta = 38.6^\circ$ for Pd/CTF confirming the presence of Pd(111). The nitrogen sorption results are consistent with former results reported by Kuhn et al.^{19–22} CTF and Pd/CTF are micro- and mesoporous and have high surface areas, over $2400 \text{ m}^2 \text{g}^{-1}$ (Table 1).

The transmission electron microscopy (TEM) (Figure 2) and scanning electron microscopy (SEM) (Figure 3) overview images of the Pd/CTF show that the Pd nanoparticles are well dispersed on the support. In Table 2, the median size of Pd nanoparticles before immobilization and immobilized on AC and CTF are shown. In both cases, a slight growing of the metal nanoparticles size during the immobilization has been observed, mainly due to aggregation of the nanoparticles. However, the Pd particles on CTF have a smaller average size and also exhibit a more homogeneous distribution when compared to Pd/AC. The catalysts were tested in the liquid phase oxidation of glycerol (glycerol solution 0.3 M and $\text{NaOH}/\text{glycerol}$ ratio = 4 mol/mol, substrate/metal 1000 mol/mol were mixed in distilled water with a total volume of 10 mL. The reactor was pressurized at 3 bar of O_2 and thermostatted at 50 °C). A first reaction using Pd-free CTF was performed in order to determine a possible activity of the Zn; no activity was observed.

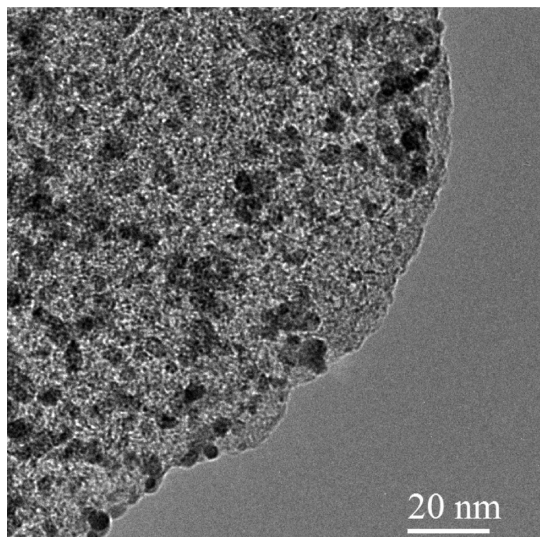


FIGURE 2. TEM image of 1 wt % Pd/CTF catalyst before reaction.

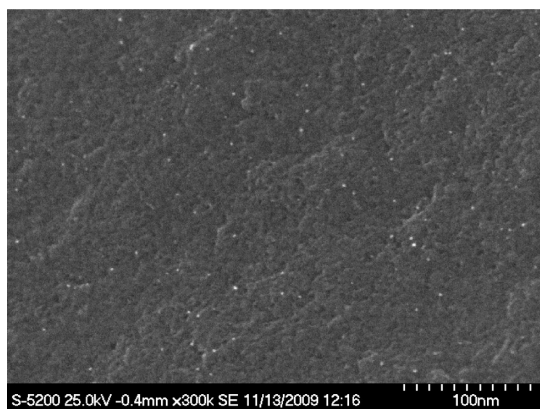


FIGURE 3. SEM image of 1 wt % Pd/CTF catalyst before reaction.

TABLE 2. Unsupported and Supported Pd Nanoparticles Size before Reaction

	statistical median (nm)	standard deviation σ
Pd colloid	2.76	0.59
Pd/AC ^a	3.94	1.15
Pd/CTF	3.08	0.73

^a Data from ref 31.

Pd/CTF showed a slightly better initial activity than Pd/AC (respectively 982 and 948 mol h⁻¹ mol⁻¹) as shown in Table 3. However the following reaction profile (Figure 4) of the two catalysts is completely different. For Pd/AC, a strong deactivation has been observed as already reported in the literature.^{25,29-31} After only three hours of reaction, glycerol was fully converted on Pd/CTF whereas the full conversion was not reached on Pd/AC. This loss of activity of Pd/AC can be addressed here to Pd aggregation as evidenced by TEM of the used catalyst (Figure 5) but also we cannot exclude metal structural modification, leaching, irreversible adsorption, overoxidation of Pd.^{25,29-31} On the contrary, Pd/CTF did not show any obvious decrease of activity. To confirm

TABLE 3. Activity and Selectivity of Pd/AC and Pd/CTF for Glycerol Oxidation^a

catalyst	initial rate ^b of consumption of glycerol (mol*h ⁻¹ *mol ⁻¹)	selectivity ^c			
		glyceric acid	tartronic acid	glycolic acid	oxalic acid
Pd/AC	948	76	6	14	4
Pd/CTF	982	81	12	4	3

^a Glycerol solution (0.3 M and NaOH/glycerol ratio = 4 mol/mol), and the catalyst (substrate/metal) 1000 mol/mol were mixed in distilled water (total volume 10 mL). The reactor was thermostated at 50 °C and pressurized at 3 bar of O₂. ^b Mols of glycerol converted divided by time and total mol of metal. ^c Calculated at 50% of conversion.

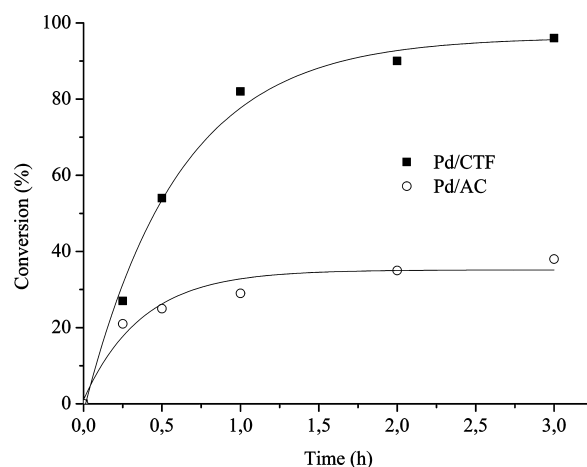


FIGURE 4. Supported Pd-based catalysts for glycerol oxidation. Glycerol solution (0.3 M and NaOH/glycerol ratio = 4 mol/mol), and the catalyst (substrate/metal) 1000 mol/mol were mixed in distilled water (total volume 10 mL). The reactor was pressurized at 3 bar of O₂ and thermostated at 50 °C.

this result a stability test of Pd/CTF, that is, recycling tests, has been performed (Figure 6). We observed a decreasing activity of the catalyst only after the fourth run, and TEM investigation (Figure 7) revealed an increase of the particles size (from 3.08 to 4.88 nm) shown in Table 4, which is accompanied by transport of the noble metal particles to the external surface of the catalyst.

However, it can be stated that Pd/CTF deactivates much slower than Pd/AC, which can be addressed to the enhanced stability of the Pd NPs by increasing the interaction with the support due to the nitrogen functionalities present in the structure of CTF. The same behavior was previously observed introducing nitrogen functionalities on the surface of CNTs.⁴⁻⁶

Strategies for a further improvement, that is, stabilization of the catalysts can thus be envisaged by introducing more heteroatoms with even higher coordination ability into the networks. Such networks could be made for example using dicyanopyridine instead of dicyanobenzene monomers,^{21,25} which is the subject of current studies.

Furthermore Pd/CTF showed a slightly better selectivity to glyceric acid than Pd/AC (respectively 81 and 76 %) but

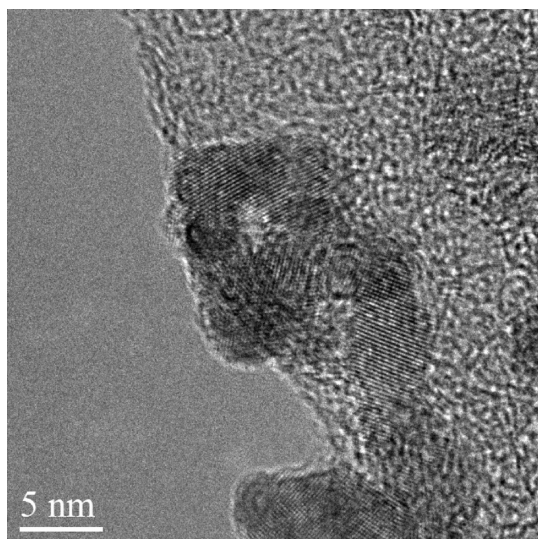


FIGURE 5. Electron micrograph of 1 wt % Pd/AC after reaction.

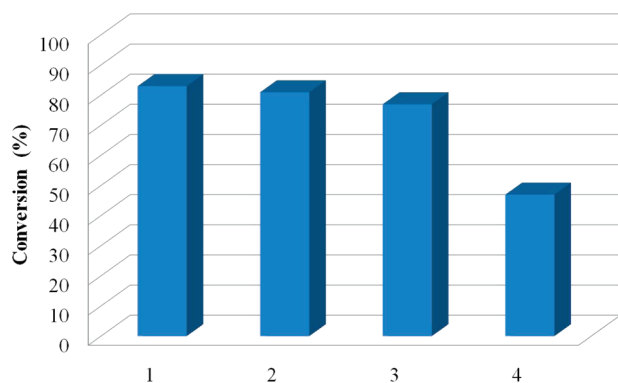


FIGURE 6. Conversion on recycling of 1% Pd/CTF. Glycerol solution (0.3 M and NaOH/glycerol ratio = 4 mol/mol), and the catalyst (substrate/metal) 1000 mol/mol were mixed in distilled water (total volume 10 mL). The reactor was pressurized at 3 bar of O₂ and thermostatted at 50 °C.

also the product distribution differs (Figure 8). In the case of the CTF catalyst, the main byproduct is the tartronic acid from the subsequent oxidation of glycerate, whereas for Pd/AC the amount of glycolic acid produced due to C–C bond cleavage increases significantly. As in any case some small amounts of Zn is remaining in the CTF structures (here 0.3 wt %) we also attempted to exclude any beneficial or detrimental effect of this residue on the catalyst performance. Therefore a second Pd/CTF catalyst was tested where the Zn content was increased deliberately to 1.3 wt % by wet impregnation of ZnCl₂. The two catalysts containing respectively 0.3 and 1.3 wt % of Zn showed the same activity; thus we can exclude any contribution of the Zn present in the support on the catalytic activity.

In summary we could conclude that Pd/CTF appeared more resistant to deactivation and more selective toward glycerate than Pd/AC. The longer lifetime of the catalyst Pd/CTF in the oxidation of glycerol can be explained by the high amount of nitrogen functionalities in the framework coor-

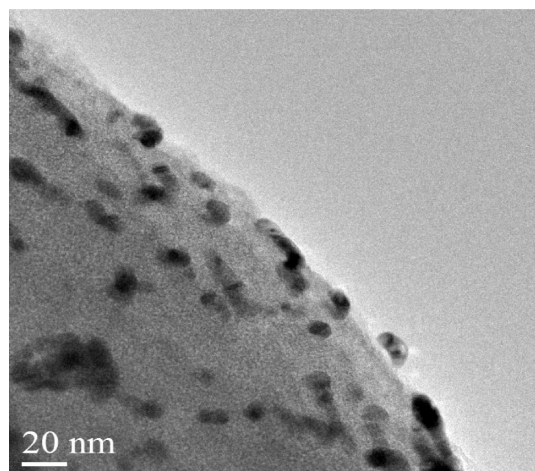


FIGURE 7. Electron micrograph of 1 wt % Pd/CTF after 4 cycles.

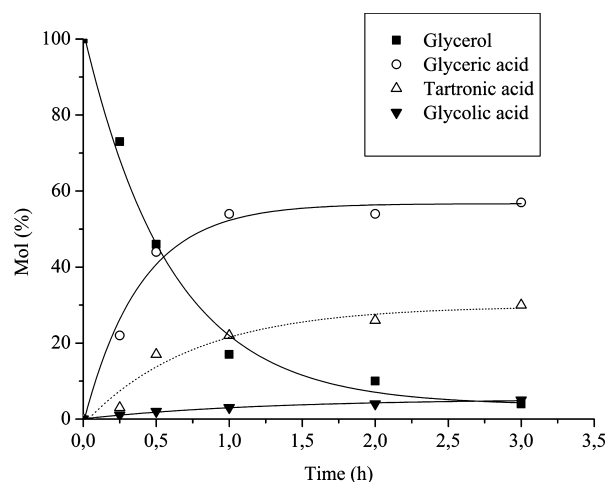


FIGURE 8. Distribution of products using Pd/CTF for glycerol oxidation. Glycerol solution (0.3 M and NaOH/glycerol ratio = 4 mol/mol), and the catalyst (substrate/metal) 1000 mol/mol were mixed in distilled water (total volume 10 mL). The reactor was pressurized at 3 bar of O₂ and thermostatted at 50 °C.

TABLE 4. Pd/CTF Particles Size before Glycerol Oxidation and after 4 Times Recycling

	statistical median (nm)	standard deviation σ
Pd/CTF before reaction	3.08	0.73
Pd/CTF after 4 cycles	4.88	1.12

dinating and thus stabilizing the metal nanoparticles and by the porous surface of the support that may offer steric restriction to confine the metal particles and thus to prevent the growth of metal clusters. Moreover the same constrains could have a beneficial effect on selectivity for the catalyst.

Acknowledgment. Financial support by the UniCat cluster of excellence (Unifying Concepts in Catalysis, Berlin) and Fondazione Cariplo are gratefully acknowledged. We thank Professor Robert Schlögl for helpful discussions. The authors would like to thank Massimo Tagliaferro from Nanovision and Paolo De Natale from Hitachi High-Technologies for the SEM images.

Supporting Information Available. Experimental part (materials and methods, synthesis), parameters of the glycerol oxidation, BET isotherms and XRD pattern of CTF and Pd/CTF. This material is available free of charge via the Internet at <http://pubs.acs.org>.

REFERENCES AND NOTES

- (1) (a) Gangwal, V. R.; van der Schaaf, J.; Kuster, B. M. F.; Schouten, J. C. *J. Catal.* **2005**, *32*, 432. (b) Hutchings, G. J.; Carrettin, S.; Landon, P.; Edwards, J. K.; Enache, D.; Knight, D. W.; Xu, Y. J.; Carley, A. F. *Top. Catal.* **2006**, *38*, 223. (c) Sheldon, R. A.; Arends, I. W. C. E.; Dijkstra, A. *Catal. Today* **2000**, *57*, 157.
- (2) Jiang, K.; Eitan, A.; Schadler, L. S.; Ajayan, P. M.; Siegel, R. W. *Nano Lett.* **2003**, *3*, 275.
- (3) Hou, X.; Wang, L.; Zhou, F.; Wang, F. *Carbon* **2009**, *47*, 1209.
- (4) Yoon, H.; Ko, S.; Jang, J. *Chem. Commun.* **2007**, 1468.
- (5) Leprò, X.; Terries, E.; Vega-Cantù, Y.; Rodriguez-Macias, F. J.; Muramatsu, H.; Ahm Kim, Y.; Hayahsi, T.; Endo, M.; Torres, R. M.; Terrones, M. *Chem. Phys. Lett.* **2008**, *463*, 124.
- (6) Amadou, J.; Chirazi, K.; Houllé, M.; Janowska, I.; Ersen, O.; Bégin, D.; Pham-Huu, C. *Catal. Today* **2008**, *138*, 62.
- (7) Jin, X.; Balasubramanian, V. V.; Selvan, S. T.; Sawant, D. P.; Chari, M. A.; Lu, G. Q.; Vinu, A. *Angew. Chem., Int. Ed.* **2009**, *48*, 1.
- (8) Farrusseng, D.; Aguado, S.; Pinel, C. *Angew. Chem., Int. Ed.* **2009**, *48*, 2.
- (9) Gascon, J.; Hernandez-Alonso, M. D.; Ameida, A. R.; van Klink, G. P. M.; Kapteijn, F.; Mul, G. *J. Catal.* **2009**, *261*, 75.
- (10) Savonnet, M.; Ravon, U.; Aguado, S.; Bazer-Bachi, D.; Lecocq, V.; Bats, N.; Pinel, C.; Farrusseng, D. *Green Chem.* **2009**, *11*, 1729.
- (11) Hermes, S.; Schroter, M.-K.; Schmid, R.; Khodeir, L.; Muhler, M.; Tissler, A.; Fischer, R. W.; Fischer, R. A. *Angew. Chem., Int. Ed.* **2005**, *44*, 6237.
- (12) Hwang, Y. K.; Hong, D.-Y.; Chang, J.-S.; Jhung, S. H.; Seo, Y.-K.; Kim, J.; Vimont, A.; Daturi, M.; Serre, C.; Férey, G. *Angew. Chem., Int. Ed.* **2008**, *47*, 4144.
- (13) (a) Moon, H. R.; Kim, J. H.; Paik Suh, M. *Angew. Chem.* **2005**, *117*, 1287. (b) Moon, H. R.; Kim, J. H.; Paik Suh, M. *Angew. Chem., Int. Ed.* **2005**, *44*, 1261.
- (14) Ishida, T.; Nagaoka, M.; Akita, T.; Haruta, M. *Chem.—Eur. J.* **2008**, *4*, 8456.
- (15) Opelt, S.; Turk, S.; Dietzsch, E.; Henschel, A.; Kaskel, S.; Klemm, E. *Catal. Commun.* **2008**, *9*, 1286.
- (16) Llabrés i Xamena, F. X.; Abad, A.; Corma, A.; Garcia, H. *J. Catal.* **2007**, *250*, 294.
- (17) Zhang, X.; Llabrés i Xamena, F. X.; Corma, A. *J. Catal.* **2009**, *265*, 155.
- (18) Sabo, M.; Henschel, A.; Froede, H.; Klemm, E.; Kaskel, S. *J. Mater. Chem.* **2007**, *17*, 3827.
- (19) Kuhn, P.; Antonietti, M.; Thomas, A. *Angew. Chem., Int. Ed.* **2008**, *47*, 3450.
- (20) Kuhn, P.; Forget, A.; Su, D. S.; Thomas, A.; Antonietti, M. *J. Am. Chem. Soc.* **2008**, *130*, 13333.
- (21) Kuhn, P.; Thomas, A.; Antonietti, M. *Macromolecules* **2009**, *42*, 319.
- (22) Kuhn, P.; Forget, A.; Hartmann, J.; Thomas, A.; Antonietti, M. *Adv. Mater.* **2009**, *21*, 897.
- (23) Palkovits, R.; Antonietti, M.; Kuhn, P.; Thomas, A.; Schüth, F. *Angew. Chem., Int. Ed.* **2009**, *48*, 1.
- (24) Carrettin, S.; McMorn, P.; Johnston, P.; Griffin, K.; Hutchings, G. J. *Chem. Comm.* **2002**, 696.
- (25) Porta, F.; Prati, L. *J. Catal.* **2004**, *224*, 397.
- (26) Ketchie, W. C.; Fang, Y.; Wong, M. S.; Murayama, M.; Davis, R. J. *J. Catal.* **2007**, *250*, 94.
- (27) Demirel-Gülen, S.; Lucas, M.; Claus, P. *Catal. Today* **2005**, *166*, 102.
- (28) Dimitratos, N.; Lopez-Sanchez, J. A.; Lennon, D.; Porta, F.; Prati, L.; Villa, A. *Catal. Lett.* **2006**, 147.
- (29) Wang, D.; Villa, A.; Porta, F.; Su, D.; Prati, L. *Chem. Comm.* **2006**, 1956.
- (30) Villa, A.; Campione, C.; Prati, L. *Catal. Lett.* **2007**, *115*, 133.
- (31) Villa, A.; Janjic, N.; Spontoni, P.; Wang, D.; Su, D. S.; Prati, L. *Appl. Catal., A* **2009**, 221.